ELSEVIER

Journal of Alloys and Compounds 408–412 (2006) 911–914

Journal of ALLOYS AND COMPOUNDS

www.elsevier.com/locate/jallcom

Luminescent properties of red long persistence phosphors, $BaMg_2Si_2O_7:Eu^{2+}$, Mn^{2+}

Sho Abe [a,*], Kazuyoshi Uematsu [b], Kenji Toda [a], Mineo Sato [b]

[a] *Graduate School of Science and Technology, Niigata University, 8050 Ikarashi 2-nocho, Niigata-shi 950-2181, Japan*
[b] *Department of Chemistry and Chemical Engineering, Niigata University, 8050 Ikarashi 2-nocho, Niigata-shi 950-2181, Japan*

Received 3 August 2004; received in revised form 13 January 2005; accepted 31 March 2005
Available online 25 July 2005

Abstract

Long persistence phosphors of $BaMg_2Si_2O_7:Eu^{2+}$, Mn^{2+} with red emission were prepared using a conventional solid state reaction. Phosphors doped only with Eu^{2+} emitted a 400 nm violet light; those doped only with Mn^{2+} emitted red light that was hardly visible. Phosphors doped with both Eu^{2+} and Mn^{2+} showed two emission peaks of 400 and 660 nm, exhibiting a reddish luminescence to the naked eye. These facts suggested an energy transfer from Eu^{2+} to Mn^{2+}. Non-stoichiometric co-doped phosphors with a deficient Ba component showed long persistence phosphorescence with reddish color.

Keywords: Long persistence phosphor; Red phosphorescence; Energy transfer; Barium magnesium silicate

1. Introduction

Long persistence phosphors are now used for clock faces and a warning lights. They continue emitting light in darkness for a long time even after ceased excitation by sunlight and fluorescent light. Recently, alkaline earth aluminates, as represented by $SrAl_2O_4:Eu^{2+}$, Dy^{3+} and $CaAl_2O_4:Eu^{2+}$, Nd^{3+}, have garnered much attention as such long persistence phosphors because they show longer persistence for light emission than conventional phosphors that are stimulated by radioactive materials [1–3]. Although these phosphors show a highly intense luminescence and a long decay time, luminescent colors are located within a comparatively narrow range that is centered upon green and blue wavelength regions. Green emissions of these phosphors, which are comfortably visible by human eyes in darkness, are sufficiently intense, but use of these phosphors remains limited to luminous paints. Therefore, long persistence phosphors that exhibit a white or multi-colored emission should be developed to expand the application of phosphors.

This study is intended to develop a reddish long persistence phosphor with the investigated luminescent properties of $BaMg_2Si_2O_7:Eu^{2+}$, Mn^{2+}. Such a phosphor is indispensable for development of white or multi-colored emission devices together with blue and green phosphors [4,5].

2. Experimental

Starting materials were $BaCO_3$ (3N; Kanto Chemical, Co. Inc.), MgO (4N; Kanto Chemical, Co. Inc.), SiO_2 (3N; Kanto Chemical, Co. Inc.), Eu_2O_3 (4N; Shinetsu Chemical Co.) and $MnCO_3$ (3N; Kojundo Chemical Laboratory Co. Ltd.); B_2O_3 (3N; Kanto Chemical, Co. Inc.) was also used as a flux. The flux concentration was fixed as 10 mol% for all experiments. Starting powders were suspended in ethanol and mixed using an agate mortar. The mixture was dried and fired in an alumina boat at 1173 K for 3 h in air. After firing, the powder sample was ground and pressed into 15-mm diameter disk-shaped pellets with ca. 1 mm thickness under a pressure of 30 MPa

* Corresponding author. Tel.: +81 25 262 6772; fax: +81 25 262 6771.
E-mail address: ktoda@eng.niigata-u.ac.jp (S. Abe).

0925-8388/$ – see front matter © 2005 Elsevier B.V. All rights reserved.
doi:10.1016/j.jallcom.2005.03.092

for 10 min. The pellet was fired in an alumina boat at 1473 K for 6 h in a slightly reductive atmosphere of 5% H_2–95% Ar gas. After firing again, the sample was ground to obtain a fine powder.

Phase identification of the samples was confirmed using a powder X-ray diffractometer (MX-Labo; Mac Science Ltd.). Powder neutron diffraction patterns were recorded using the HERMES (T1-3) diffractometer installed at JRR-3M Guide Hall in the Japan Atomic Energy Research Institute (JAERI) [6]. An incident neutron wavelength of $\lambda = 0.182035$ nm was obtained from a Ge(3 1 1) monochromator. Data were collected for thoroughly ground powders using multi-scanning mode in the 2θ range from 5° to 155° with a 0.1° step width and a 16 min monitoring time. Powder patterns obtained were analyzed using the RIETAN2000 profile refinement program [7]. The excitation and emission spectra were measured for the powder sample using a spectrofluorometer (FP-6500/6600; Jasco Inc.). The chromaticity coordinates for powder samples were measured using a (PMA-11; Hamamatsu Photonics Inc.) equipped with an 11 W UV lamp.

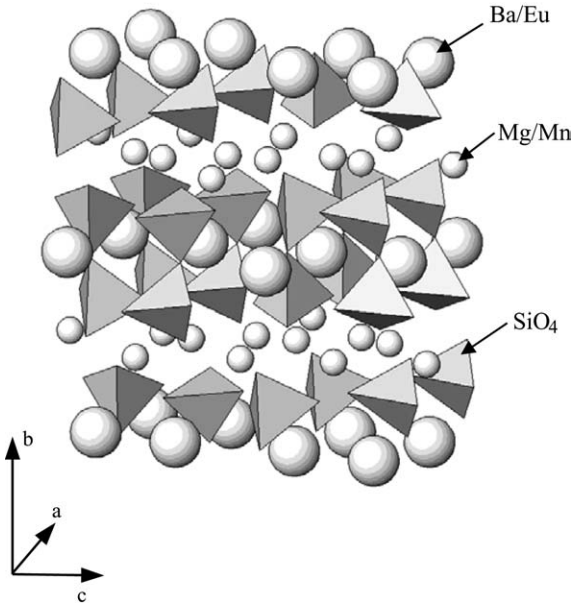

Fig. 2. Crystal structure of $BaMg_2Si_2O_7:Eu^{2+}$, Mn^{2+}.

3. Results and discussion

Powder X-ray diffraction measurements revealed that the crystal structure of all prepared samples was $BaCo_2Si_2O_7$, as reported by Adams et al., with low temperature phase of $BaZn_2Si_2O_7$ [8,9]. The $Ba_{0.99}Mg_{1.8}Si_2O_7:Eu_{0.01}$, $Mn_{0.2}$ structure was refined by Rietveld analysis for the neutron diffraction data using structural parameters of $BaCo_2Si_2O_7$. Fig. 1 shows the Rietveld refinement profile of the neutron diffraction data. The structure belongs to a monoclinic space group $C12/c1$; the lattice constants refined were $a = 0.72529(2)$ nm, $b = 1.27345(5)$ nm, $c = 1.37846(5)$ nm and $\beta = 90.213(3)°$. A structural model in which manganese atoms were assigned to the three magnesium sites with an equimolar ratio as a mixed species gave the most reasonable refinement, resulting in 3.46% for the R_{wp} factor. Detailed oxygen positional data revealed that the Mg site was a distorted octahedron. The Eu atom concentration was quite small (1 mol%). Therefore, all assignments of Eu to Ba or Mg sites showed insignificant influence. From a crystallographic viewpoint, Eu atoms were inferred to be located on the Ba site. That structure is shown in Fig. 2.

Fig. 3 shows excitation and emission spectra of $Ba_{0.99}Mg_2Si_2O_7:Eu_{0.01}$ (a), $BaMg_{1.8}Si_2O_7:Mn_{0.2}$ (b) and $Ba_{0.99}Mg_{1.8}Si_2O_7:Eu_{0.01}$, $Mn_{0.2}$ (c). Phosphors doped only with Eu^{2+} emitted a 400 nm violet light; those doped only with Mn^{2+} emitted a red light that was hardly visible. The violet light and the red light are attributed to the 4f–5d transition of Eu^{2+} and the $^4T_1 \rightarrow {}^6A_1$ transition of Mn^{2+} [10], respectively. On the other hand, phosphors doped both with Eu^{2+}

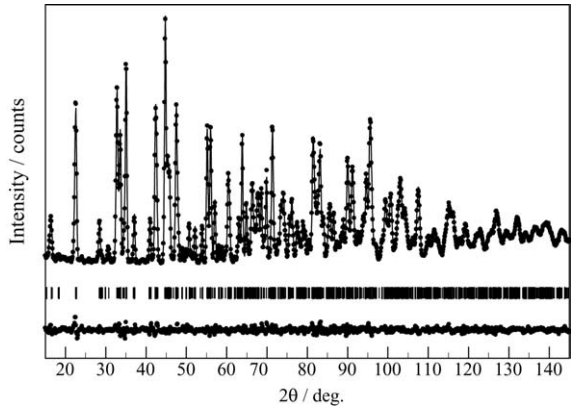

Fig. 1. Rietveld refinement profile of neutron diffraction data for $Ba_{0.99}Mg_{1.8}Si_2O_7:Eu_{0.01}$, $Mn_{0.2}$. The dotted line is observed pattern and the solid line represents the calculated pattern. Vertical marks in the middle show positions calculated for Bragg reflections. The trace on the bottom indicates the differences between the calculated and observed intensities.

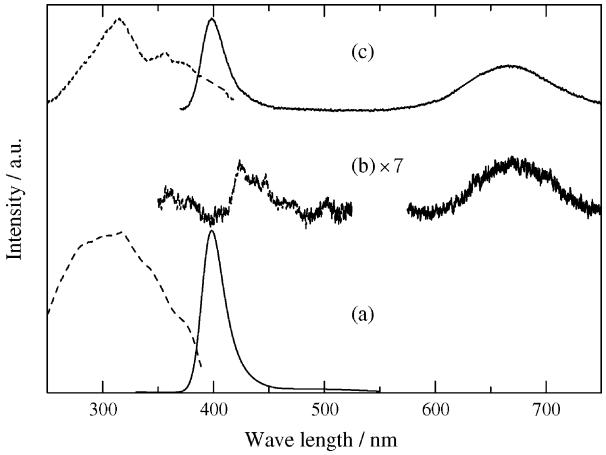

Fig. 3. Excitation (dotted line) and emission (solid line) spectra of $Ba_{0.99}Mg_2Si_2O_7:Eu_{0.01}$ (a), $BaMg_{1.8}Si_2O_7:Mn_{0.2}$ (b) and $Ba_{0.99}Mg_{1.8}Si_2O_7:Eu_{0.01}$, $Mn_{0.2}$ (c).

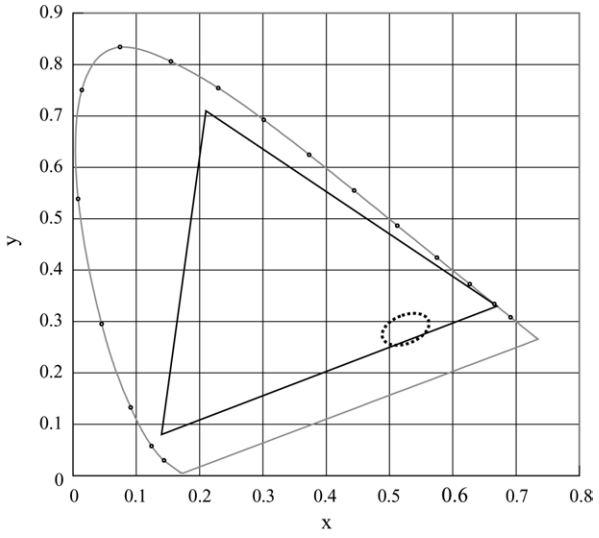

Fig. 4. Chromaticity diagram of $BaMg_2Si_2O_7:Eu^{2+}$, Mn^{2+} emission.

and Mn^{2+} showed two emission peaks of 400 and 660 nm, exhibiting a reddish luminescence to the naked eye. The red emission peak of 660 nm is similar to the weak emission, which is usually observed in phosphors doped only with Mn^{2+}. It is noteworthy that the emission intensity of (c) is seven times higher than that of (b). These facts strongly suggest an energy transfer from Eu^{2+} to Mn^{2+}. Fig. 4 shows the emission color of $BaMg_2Si_2O_7:Eu^{2+}$, Mn^{2+} in the chromaticity diagram. The emission color varies with the concentration of Eu^{2+} and Mn^{2+} in the range surrounded by the dotted line.

Interestingly, the phosphors doped only with Eu^{2+} showed a small but certain amount of afterglow. This fact implies that the phosphors doped both with Eu^{2+} and Mn^{2+} show a red afterglow because Mn^{2+} receives energy from Eu^{2+} continuously. Both the afterglow intensity and the decay time, however, decreased remarkably as the quantity of doped Mn^{2+} ion increased. The afterglow became invisible at doping concentrations greater than 10 mol% of Mg^{2+}. In $SrAl_2O_4:Eu^{2+}$, Dy^{3+}, $Sr_2MgSi_2O_7:Eu^{2+}$, Dy^{3+} and $CaAl_2O_4:Eu^{2+}$, Nd^{3+}, known as famous long persistence phosphors, the Dy^{3+} and Nd^{3+} dopants serve as intensifiers to increase the afterglow intensity [11]. These rare earth ions are considered to create oxygen defects or cation defects. According to Ohta et al., a Sr (Ca) defect functions as an electron hole trap that is stabilized by Dy^{3+} (Nd^{3+}), thereby providing a remarkable increase in afterglow intensity [12,13]. We attempted to improve the afterglow characteristic by means of making the sample composition non-stoichiometric. We prepared various samples with matrix components that deviated from stoichiometry. In samples whose Ba content was slightly deficient from stoichiometry (Ba-poor samples), the afterglow became intense in the initial stage of afterglow, but the luminescence intensity decreased slightly. Ba cation defects or oxygen defects may be generated in the Ba-poor samples, thereafter functioning as a trap for holes or electrons. Fig. 5 shows the afterglow decay curves for the stoichiometric sample of $Ba_{0.99}Mg_{1.8}Si_2O_7:Eu_{0.01}$, $Mn_{0.2}$ (d) and the non-stoichiometric Ba-poor sample (e). Dependence of the initial afterglow intensity on the Ba deficiency is shown in Fig. 6. This result implies that generation of Ba cation defects or oxygen defects are responsible for the increase in the initial afterglow intensity. The defect identification produced by the Ba deficiency is important for elucidating the afterglow mechanism observed in these phosphors. Details of this defect identification are under examination.

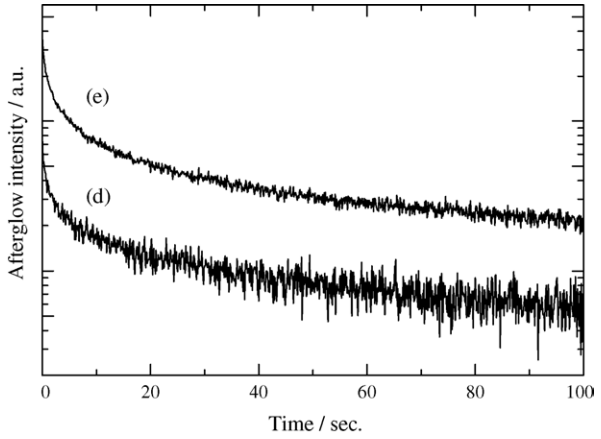

Fig. 5. Afterglow decay curves for a stoichiometric sample of $Ba_{0.99}Mg_{1.8}Si_2O_7:Eu_{0.01}$, $Mn_{0.2}$ (d) and non-stoichiometric Ba-poor (20%) sample (e). The decay curve was monitored at around 660 nm after excitation from a Xe lamp for 3 min.

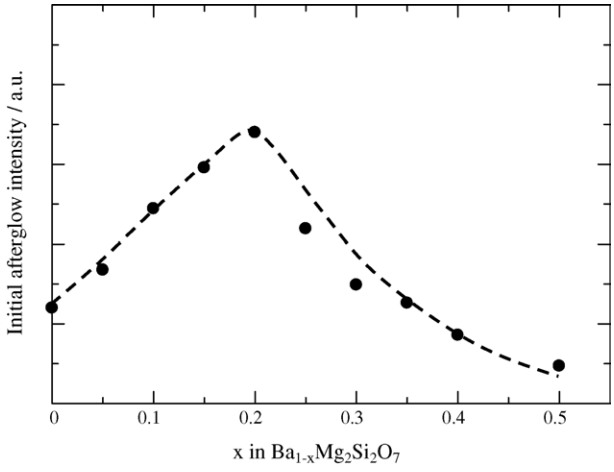

Fig. 6. Dependence of initial afterglow intensity on the Ba deficiency in $Ba_{1-x}Mg_2Si_2O_7$.

4. Conclusion

$BaMg_2Si_2O_7:Eu^{2+}$, Mn^{2+} was prepared as a red long persistence phosphor using a conventional solid state reaction. Phosphors doped only with Mn^{2+} emitted a red light that was barely visible. Phosphors doped with both Eu^{2+} and Mn^{2+} showed a reddish luminescence. In addition, the red emission intensity of co-doped sample was seven times higher

than that doped only with Mn^{2+}. These facts suggest an energy transfer from Eu^{2+} to Mn^{2+}. The co-doped phosphor showed a reddish luminescence and phosphorescence, but the increase of doped Mn^{2+} concentration engendered a decrease in afterglow intensity and decay time. However, a non-stoichiometric co-doped phosphor with a Ba component deficiency showed higher initial afterglow intensity. This fact indicates that the defects, probably Ba cation or oxygen vacancies, introduced by the deficiency of Ba component are strongly correlated with the afterglow.

References

[1] T. Matsuzawa, N. Takeuchi, Y. Aoki, Y. Murayama, The 248th Meeting Technical Digest, Phosphor Research Society, 1993, pp. 7–13.
[2] Y. Murayama, Nikkei Sci. 26 (1996) 20–29.
[3] T. Matsuzawa, Y. Aoki, N. Takeuchi, Y. Murayama, J. Electrochem. Soc. 143 (1996) 2670–2673.
[4] T.L. Barry, J. Electrochem. Soc. 117 (1970) 381–385.
[5] G.Q. Yao, J.H. Lin, L. Zhang, G.X. Lu, M.Z. Gong, Su, J. Matter. Chem. 8 (1998) 585–588.
[6] K. Ohyama, T. Kanouchi, K. Nemoto, M. Ohashi, T. Kajitani, Y. Yamaguchi, Jpn. J. Appl. Phys. 37 (1998) 3319–3326.
[7] F. Izumi, T. Ikeda, Mater. Sci. Forum 321–324 (2000) 198.
[8] R.D. Adams, R. Layland, Polyhedron 12 (1993) 2075.
[9] J.H. Lin, G.X. Lu, J. Du, M.Z. Su, C.K. Loong, J.W. Richardson, J. Phys. Chem. Solids 60 (1999) 975–983.
[10] G. Blasse, A. Bril, Phillips Tech. Rev. 31 (1970) 304.
[11] K. Toda, Y. Imanari, T. Nonogawa, J. Miyoshi, K. Uematsu, M. Sato, J. Ceram. Soc. Jpn. 110 (2002) 283–288.
[12] M. Ohta, M. Maruyama, T. Nishijo, Kidorui 36 (2000) 244–245.
[13] M. Ohta, M. Maruyama, T. Hayakawa, T. Nishijo, J. Ceram. Soc. Jpn. 108 (2000) 284–289.